Electric Power Systems Research 213 (2022) 108749

Contents lists available at ScienceDirect

Electric Power Systems Research

journal homepage: www.elsevier.com/locate/epsr

Potential of Mobile Energy Hubs for Enhancing Resilience of Electricity Distribution Systems

Amid Shahbazi [a], Jamshid Aghaei [a,b,*], Taher Niknam [a], Masood Ardeshiri [a], Abdollah Kavousi-Fard [a], Miadreza Shafie-khah [c]

[a] Department of Electrical and Electronics Engineering, Shiraz University of Technology, Shiraz, Iran
[b] Department of Electrical Engineering, School of Energy Systems, Lappeenranta University of Technology, Lappeenranta, Finland
[c] School of Technology and Innovations, University of Vaasa, Vaasa, Finland

ARTICLE INFO

Keywords:
Resilience
Distributed Generation
Short Path Algorithm
Mobile Energy Hub
Electricity distribution systems

ABSTRACT

In this paper, an operational framework is presented to improve electrical distribution network resilience based on the Mobile Energy Hubs (MEHs) concept. In fact, critical loads should be immediately islanded in a post-flood state and then recovered. Accordingly, this paper focuses on providing an effective management solution to enhance the functioning of electricity distribution systems with the objective of maximizing restoration of critical loads and minimizing their restoration time span based on MEH. To this end, MEHs are installed on trucks to deliver the required power for supplying the islanded critical loads in zones affected by a flood. Besides, in order to demonstrate a practical resilient structure, possible damage inflicted on other critical infrastructures is considered. Moreover, obstacles resulting from the destruction of the transportation infrastructure caused by a flood are overcome by using the shortest path algorithm (SPA). In this case, the optimization algorithm determines the shortest possible path for transporting the MEHs to supply critical loads in the least time aiming to improve the network resilience indicators. Finally, the proposed framework is studied in a standard test electricity distribution network. Simulations are carried out to evaluate the network resilience indicators of the proposed framework in obtaining a resilient distribution network during natural disasters.

1. Introduction

Adverse weather events and natural disasters caused by climate change, in particular severe floods, can lead to serious problems in electricity distribution systems, such as long-term disconnection of critical loads, a low quality of power transmission, and an increase in economic losses [1]. Currently, many electricity distribution systems are designed for normal weather conditions, which means that their resilience is low or zero to extensive damage caused by natural disasters [2]. For instance, over ten thousand pieces of equipment of the electricity distribution system were damaged as a result of adverse weather events in Florida in 2005 [2]. In the USA, over 80% of power outages between 2003 and 2012 were caused by weather conditions [3]. Over USD 1 billion of financial damage was due to eight weather-related events, including floods and blizzards that occurred in the first six months of 2016 [4]. Moreover, Hurricane Sandy was another severe natural disaster that inflicted serious damage on the power system in the USA. It caused a power outage of 5.7 million customers in 15 states when hitting the east coasts of the country [5]. It should also be noted that severe storms caused damage worth more than USD 1 billion in China in 2008; 2000 distribution substations were disconnected and over 8500 occurrences of damage happened on medium and low voltage networks [6]. Therefore, based on research on recent severe natural incidents, the concept of power network resilience has been introduced in the electrical industry to alleviate and tackle the adverse effects of weather events on electric power systems. The term “resilience” refers to enhancing the stability of the system against incidents with a high impact and a low probability and its capability of rapid restoration after the event. It is worth mentioning that such adverse events can be life-threatening and cause disruption in generation, transmission, and distribution systems also in integrated systems, such as fuel and natural gas transportation and telecommunication systems [7].

In recent years, various procedures have been presented to enhance the resilience of electric power networks in studies on the resilience analysis of power networks [8–9]. In [10], distributed generator (DG) resources along with a model of distribution systems were considered for restoration of substantial loads in adjacent buses of DGs. Furthermore,

* Corresponding author.
E-mail address: jamshid.aghaei@lut.fi (J. Aghaei).

https://doi.org/10.1016/j.epsr.2022.108749
Received 22 December 2021; Received in revised form 27 April 2022; Accepted 20 August 2022
Available online 27 August 2022

Nomenclature

A. Sets/Indices

Ω^{L} Index of distribution lines.
Ω^{TL} Index of transportation lines.
Ω^{B} Index of distribution system buses ($\Omega^{BG} \cup \Omega^{BS} \cup \Omega^{BMG}$).
Ω^{T} Time index.
s The first location of each MEH.
Ω^{B} Set of transportation nodes.
Ω^{Δ} Index for the weights of the roads.
Ω^{J} Index of node classification.
λ Piecewise linearization index.

B. Constants

CT^{S}_{m}, DT^{S}_{m} Minimum charging and discharging time (hr).
$\underline{C^{S}_{m}}, \overline{C^{S}_{m}}$ Minimum and maximum allowable stored energy (kWh).
$\overline{I^{L}}$ Maximum current of lines flow (A).
$\underline{P^{Ch}_{m}}, \overline{P^{Ch}_{m}}$ Minimum and maximum amount of EH charging power (kW).
$\underline{P^{Disch}_{m}}, \overline{P^{Disch}_{m}}$ Minimum and maximum amount of EH discharging power (kW).
$\underline{P^{G}_{m}}, \overline{P^{G}_{m}}$ Minimum and maximum amount of active generation power of DG units (kW).
$\underline{P^{MEH}_{n}}, \overline{P^{MEH}_{n}}$ Minimum and maximum amount of active generation power of MEHs (kW).
$\overline{P^{MG}_{l}}, \overline{Q^{MG}_{l}}$ Maximum amount of reactive and active generation power of the DS (kW).
$\underline{Q^{G}_{m}}, \overline{Q^{G}_{m}}$ Minimum and maximum amount of reactive power generation of DGs (kVAr).
$\underline{Q^{MER}_{n}}, \overline{Q^{MER}_{n}}$ Minimum and maximum amount of reactive power generation of MEHs (kVAr).
Z_{mn} Total impedance of lines (ohm).
RU^{G}_{m}, RD^{G}_{m} Ramp-up and ramp-down power rate of each DG unit (kW).
T^{O} Time period of load restoration.
$\eta^{Ch}_{m}, \eta^{Disch}_{m}$ Charging and discharging EH battery efficiency.
ρ^{G}_{m} Cost of DG generation power ($/kW).

C. Variables

$C^{S}_{m,t}$ Energy stored in an energy storage unit.
$I^{L}_{mn,t}$ Current flow of distribution lines (A).
$P^{Ch}_{m,t}, P^{Disch}_{m,t}$ Charging and discharging power (kW).
$P^{D}_{m,t}, Q^{D}_{m,t}$ Active and reactive power demand (kW and kVAr).
$P^{L}_{mn,t}, Q^{L}_{mn,t}$ Active and reactive power flow of distribution lines (kW and kVAr).
$P^{G}_{m,t}, Q^{G}_{m,t}$ Active and reactive power generation of each DG unit (kW and kVAr).
$P^{M}_{l,t}, Q^{M}_{l,t}$ Active and reactive power of an adjacent DS (kW and kVAr).
$P^{MEH}_{n,t}, Q^{MEH}_{n,t}$ Active and reactive power of MEHs (kW and kVAr).
$T^{Ch}_{m,t}, T^{Disch}_{m,t}$ Number of successive charging and discharging hours (h).
$x^{MEH}_{n,t}$ Binary variable that indicates if MEH is available at node n at time t or not.
$\overline{x}^{MEH}_{t}$ Maximum truck mounted MEHs.
$y^{Ch}_{m,t}, y^{Disch}_{m,t}$ Charging and discharging status of an EH energy storage.

Table 1
Brief comparison of [16]–[22].

Reference	Considering Energy Hub	Considering DG	Considering transportation infrastructures	Considering Shortest Path algorithm (SPA)
[16]	×	✓	×	×
[17]	×	✓	×	×
[18]	×	✓	✓	×
[19]	×	×	✓	×
[20]	×	✓	✓	×
[21]	×	✓	✓	×
[22]	✓	✓	×	×
Proposed Model	✓	✓	✓	✓

the idea of using distribution systems was provided in [11] to reduce the congestion level of feeders in regions experiencing a power outage. All the damaged loads in the critical zones will be supplied through the free capacity of the distribution system. In [12], a mixed-integer linear programming (MILP) method was formulated to determine the restoration sequence of failed components to maximize the resilience of the electricity distribution system. An effective algorithm in electricity distribution systems was proposed in [13] to support critical loads by using multiple DGs after extreme events. In this paper, the authors used a public communication platform to handle the local connection and DGs coordination after the occurrence of an adverse event. A new strategy was provided in [14] to carry out DG operation in normal and critical conditions. Maximization of the profit of the network is the objective function in the normal operating situation, and also ensuring the continuous supply of network loads is the target in critical situations. Possible ways to exploit electricity distribution systems as means to enhance network resilience and the advantages and technical challenges of these methods were discussed in [15].

The authors of [16] presented an approach based on Mobile Power Sources (MPSs), where electric means of transportation, an itinerant storage source installed on trucks, and a mobile emergency generator were used as efficient tools to boost the resilience of the distribution system (DS) during severe natural incidents.

In [17], the concept of resilience in electricity distribution systems was presented. A novel two-stage stochastic method based on MILP was proposed to evaluate the resilience of distribution systems. In [18], a plan for the restoration of vital loads was proposed by adopting a dispatch technique for mobile power sources (MPSs) and repair services (RSs). Furthermore, the cell transmission model (CTM) was employed to formulate the problem of weight dynamic traffic assignment (WDTA) in the transportation system (TS) as a linear program (LP), with the objective of the prioritized minimization of MPSs and RS. The mutual dependence of the critical substructures in restoring the electric loads of the customers has been investigated and analyzed after the occurrence of natural events in [19–20]. In [21], the authors improved the networked microgrid resilience after a hurricane by taking into account the mobile emergency resources and applying a two-stage stochastic reconfiguration strategy. It is worth noting that all the above papers only focused on electricity distribution networks and did not investigate damage on other critical substructures, such as roads. Obviously, it is necessary also to consider the damage inflicted on other substructures to provide a truly resilient structure. One of the significant problems of the previous studies is the lack of linkage between transportation infrastructures, such as roads, in critical conditions to supply the critical loads. The Energy Hub (EH) is a multicarrier power technology that involves multiple sources and functions deploying various gas, heat, and electricity conversion technologies and effective methodologies to meet domestic, commercial, and industrial power demand [22]. Furthermore, considering the connection between substructures of the transportation infrastructure and the electric power network is a notable issue in the field of critical load restoration, which is investigated in this paper by using Mobile Energy Hubs (MEHs), as some routes would become inaccessible after a flood. Table 1 summarizes the above approaches.

Considering the above approaches, the main novelties of this paper can be listed as follows:

- Developing an effective and practical multicarrier energy structure to enhance the resilience of electricity distribution systems after severe floods.
- Proposing mobile emergency energy hubs to manage the problem of supporting critical loads after a natural disaster; the hubs are implemented on trucks, and the shortest path for such mobile systems to reach the critical loads is determined.
- Analyzing the relation between the power system load flow and the transportation infrastructure after natural events in order to enhance the resilience of power systems in the presence of a multicarrier energy system.

This paper is divided into sections as follows: In Section 2, the problem formulation related to the aforementioned structure is provided. Section 3 describes the algorithm to find the shortest paths available for mobile trucks. Section 4 focuses on flood modeling on a target distribution system and discusses the results of the proposed model. Finally, conclusions are drawn in Section 5.

2. Problem formulation and component modeling

This section investigates the problem formulation including the constraints and objective functions related to the problem of network resilience. In addition, modeling of the distribution system and its equipment with the objective of improving the network resilience is presented in this section.

2.1. Problem Objective Function

Basically, the objective function of the problem is maximization of the system resilience in the load restoration process by using portable emergency EHs, which consist of a combined heat and power (CHP) unit and an electrical battery. It should be mentioned that the input of the EHs can be natural gas or biofuel, which is converted into electrical or heating power.

F(t) represents the function of system operation in various times, such as during flood events *te-tpe*, network destruction as a result of a flood *tpe-tr*, network restoration state *tr-tpr*, the situation after network restoration *tpr-tir*, and restoration of the substructure *tir-tpi* [23].

It is worth mentioning that the MEHs are assigned to the most appropriate regions in flood path for immediate power delivery to the damaged locations based on satellite big data before the flood [24]. The time period *tr-tir* is known as the most significant time after severe floods when considering improvement of the system resilience; this time period is related to the network restoration state and also the period after network restoration. Further, to supply the critical loads, the strategy of network restoration should be implemented within this period. In addition, the duration of the power outage can be estimated after the flood by prediction methods and based on network operators' experience of the distribution network. Nevertheless, the network restoration strategy must be performed during *tr-(tr+T)*. After that, the daily operation of the electrical industry will begin to supply loads. The resilience of the system after a flood (time period related to the optimization of the placement of the mobile energy hub) can be calculated by an integral function of the system performance during the aforementioned time period minus expenses assigned to the sources [23].

$$R = \gamma \times \int_{t_r}^{t_r+T^0} F(t)dt - C_G \tag{1}$$

In (1), R is an index of system resilience within the considered interval *tr-(tr+T)* of integration. Hence, maximizing R leads to the maximization of *F(t)* or minimization of the expenses allocated to the presence of distribution generation in the power network (C_G) or improvement of the system resilience. The parameter γ is defined to transform the amount of energy to its cost value. Furthermore, the term of the performance of the system *F(t),* Eq. (2), is based on the energy needed for the critical loads according to their weighting priority [23].

$$F(t) = \sum_{\forall m \in \mho^B} W_m P^D_{m,t}, \quad t \in \left[t_r, t_r + T^0\right] \tag{2}$$

Hence, the resilience index of the system can be updated and changed by considering T^{CL} as the service provided to critical loads after a severe flood and a function of the system operation in this period. The proposed alteration is provided as follows:

$$\begin{aligned} R &= \gamma \times \int_{t_r}^{t_r+T^0} \left(\sum_{\forall m \in \mho^B} W_{m,t} P^D_{m,t}\right) dt - C_G = \gamma \times \sum_{\forall m \in \mho^B} W_m \int_{t_r}^{t_r+T^0} P^D_{m,t} dt - C_G \\ &= \gamma \times \sum_{\forall m \in \mho^B} W_m \int_{t_r}^{t_r+T^{CL}} P^D_{m,t} dt - C_G = \gamma \times \sum_{\forall m \in \mho^B} W_m P^D_m T^{CL}_m - C_G \end{aligned} \tag{3}$$

In the above-mentioned equations, T^{CL} is calculated based on the computation of the time that portable EHs take to reach the critical loads. On the other hand, the term C_G in (3) represents the rate of allocation of the expenses of the distribution generation aiming to restore the distribution system with a lower number of distribution generation units as shown in Eq. (4).

$$C_G = \sum_{t \in \mho^T} \left(\sum_{m \in \mho^{BG}} \rho^G_m P^G_{m,t} + \sum_{n \in \mho^{BMG}} \rho^{MEH}_n P^{MEH}_{n,t} \right) \delta \tag{4}$$

2.2. Modeling the constraints of the problem components

The constraints related to the distribution system modeling are provided in (5)–(17). Constraints (5)–(10) are associated with dispatchable DGs in the network, and constraints (11)–(17) are related to the modeling of mobile EH resources installed on trucks located in the distribution systems. Moreover, limitation of active and reactive powers of the distribution generation units is given by (5)–(6).

$$\underline{P^G_m} x^G_{m,t} \le P^G_{m,t} \le \overline{P^G_m} x^G_{m,t}, \qquad \forall m \in \mho^{BG}, \forall t \in \mho^T \tag{5}$$

$$\underline{Q^G_m} x^G_{m,t} \le Q^G_{m,t} \le \overline{Q^G_m} x^G_{m,t}, \qquad \forall m \in \mho^{BG}, \quad \forall t \in \mho^T \tag{6}$$

Furthermore, the start-up and shut-down rates of the distributed generation units are provided in (7) and (8), respectively.

$$P^G_{m,t} - P^G_{m,t-1} \le RU^G_m, \qquad \forall m \in \mho^{BG}, \forall t \in \mho^T \tag{7}$$

$$P^G_{m,t-1} - P^G_{m,t} \le RD^G_m, \qquad \forall m \in \mho^{BG}, \forall t \in \mho^T \tag{8}$$

The minimum times that the DG sources must be in service or out of service are expressed by constraints (9)–(10).

$$T^{G-on}_{m,t} \ge UT^G_m \left(x^G_{m,t} - x^G_{m,t-1}\right), \qquad \forall m \in \mho^{BG}, \forall t \in \mho^T \tag{9}$$

$$T^{G-off}_{m,t} \ge DT^G_m \left(x^G_{m,t-1} - x^G_{m,t}\right), \qquad \forall m \in \mho^{BG}, \quad \forall t \in \mho^T \tag{10}$$

Constraints (11)–(12) determine the upper and lower bounds over the output of MEHs.

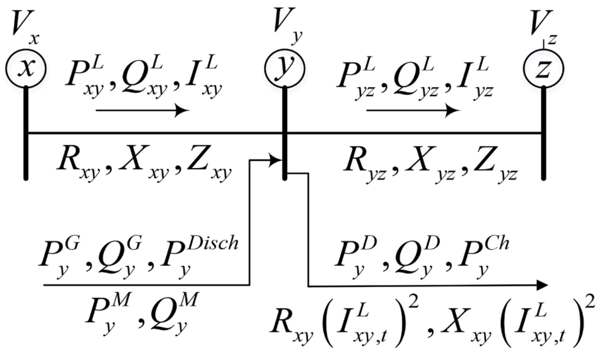

Fig. 1. Presentation of a radial distribution network.

$$\underline{P_n^{MEH}} x_{n,t}^{MEH} \le P_{n,t}^{MEH} \le \overline{P_n^{MDG}EH} x_{n,t}^{MEH}, \qquad \forall n \in \mho^{MEH}, \forall t \in \mho^T \tag{11}$$

$$\underline{Q_n^{MEH}} x_{n,t}^{MEH} \le Q_{n,t}^{MEH} \le \overline{Q_n^{MEH}} x_{n,t}^{MEH}, \qquad \forall n \in \mho^{MEH}, \ \forall t \in \mho^T \tag{12}$$

The minimum charge and discharge rates of the MEHs are demonstrated in the following equations.

$$\underline{P_m^{Ch}} y_{m,t}^{Ch} \le P_{m,t}^{Ch} \le \overline{P_m^{Ch}} y_{m,t}^{Ch}, \qquad \forall m \in \mho^{BS}, \ \forall t \in \mho^T \tag{13}$$

$$\underline{P_m^{Disch}} y_{m,t}^{Disch} \le P_{m,t}^{Disch} \le \overline{P_m^{Disch}} y_{m,t}^{Disch}, \qquad \forall m \in \mho^{BS}, \ \forall t \in \mho^T \tag{14}$$

The range of accessible energy level is shown by (15) and (16).

$$C_{m,t}^S = C_{m,t-1}^S - \frac{P_{m,t}^{Disch}\delta}{\eta_m^{Disch}} + P_{m,t}^{Ch}\delta\eta_m^{Ch}, \forall m \in \mho^{BS}, \forall t \in \mho^T \tag{15}$$

$$\underline{C_m^S} \le C_{m,t}^S \le \overline{C_m^S}, \qquad \forall m \in \mho^{BS}, \ \forall t \in \mho^T \tag{16}$$

Further, the minimum times of charge and discharge of the EH are given by (17)–(18).

$$T_{m,t}^{Ch} \ge CT_m^S\left(y_{m,t}^{Ch} - y_{m,t-1}^{Ch}\right), \qquad \forall m \in \mho^{BS}, \quad \forall t \in \mho^T \tag{17}$$

$$T_{m,t}^{Disch} \ge DT_m^S\left(y_{m,t}^{Disch} - y_{m,t-1}^{Disch}\right), \qquad \forall m \in \mho^{BS}, \quad \forall t \in \mho^T \tag{18}$$

Constraint (19) determines that the charge and discharge state of the EHs cannot be performed simultaneously. Further, the maximum number of available EHs in the distribution system for rapid supply of the demand loads on the network is provided by constraint (20).

$$y_{m,t}^{Ch} + y_{m,t}^{Disch} \le 1 \qquad \forall m \in \mho^{BS}, \ \forall t \in \mho^T \tag{19}$$

$$\sum_n x_{n,t}^{MEH} \le \bar{x}_t^{MEH} \qquad \forall t \in \mho^T \tag{20}$$

2.3. Model of the Electricity Distribution System

This section presents a linear steady-state model for the power distribution grid. The proposed model consists of the mathematical relations of the power flow for the modeling of active and reactive power loads. Moreover, it recognizes the islanded buses with the sum of power required to recover them. Eqs. (21)–(29) represent the AC model of power flow in a distribution system according to a set of recursive mathematical relations, which are illustrated in Fig. 1. In these relations, the positions of MEHs and the required capacities are characterized; they will be used further to deliver power by the MEHs of mobile trucks. Eqs. (21)–(22) give both the active and reactive power balances of the buses of the distribution system, including all DGs, MEHs, and demands.

$$\sum_{xy \in \Omega^L}\left[P_{xy}^L - R_{xy}\left(I_{xy,t}^L\right)^2\right] - \sum_{yz \in \Omega^L} P_{yz,t}^L + P_{y,t}^G + P_{z,t}^{MEH} - P_{y,t}^{Ch} + P_{y,t}^{Disch} + \sum_{x \in \Omega^{MG}} P_{x,t}^M = P_{x,t}^D$$
$$\forall y \in \Omega^B, \forall z \in \Omega^{MEH}, \forall t \in \Omega^T \tag{21}$$

$$\sum_{xy \in \Omega^L}\left[Q_{xy,t}^L - X_{xy}\left(I_{xy,t}^L\right)^2\right] - \sum_{yz \in \Omega^L} Q_{yz,t}^L + Q_{y,t}^G + Q_{z,t}^{MEH} + \sum_{x \in \Omega^{MG}} Q_{x,t}^M = Q_{y,t}^D$$
$$\forall y \in \Omega^B, \ \forall z \in \Omega^{MEH}, \forall t \in \Omega^T \tag{22}$$

In the above equation, $P_{y.t}^M / Q_{y.t}^M$ demonstrates the rate of active and reactive powers exchanged between the distribution system and a utility. Kirchhoff's voltage law (KVL) is provided in (23)–(24), which are related to the lines of the distribution system. In this case, an auxiliary variable is shown with $\Delta V_{yz.t}$, which is zero if the line yz is shifted on the distribution system at each time slot, otherwise it is either positive or negative.

$$(V_{y,t})^2 - (V_{z,t})^2 = 2\left(R_{yz}P_{yz,t}^L + X_{yz}Q_{yz,t}^L\right) - (Z_{yz})^2\left(I_{yz,t}^L\right)^2 + \Delta V_{yz,t} \qquad \forall yz \in \Omega^L, \ \forall t \in \Omega^T \tag{23}$$

$$(V_{y,t})^2\left(I_{yz,t}^L\right)^2 = \left(P_{yz,t}^L\right)^2 + \left(Q_{yz,t}^L\right)^2 \qquad \forall yz \in \Omega^L, \ \forall t \in \Omega^T \tag{24}$$

The desirable value of the bus voltage magnitude is presented in (25).

$$\underline{V} \le V_{y,t} \le \overline{V} \qquad \forall y \in \Omega^B, \forall t \in \Omega^T \tag{25}$$

The maximum current flow capacity of the feeder is shown in (26). Again, if it is zero, would indicate that the line is out of service. The variable of the binary $w_{yz.t}^L$ is equal to 1 only if the line of relevant distribution is truly working; otherwise, its value would be zero, which are provided in Eqs. (26) and (27) as follows:

$$0 \le I_{yz,t}^L \le \overline{I^L} w_{yz,t}^L \qquad \forall yz \in \Omega^{DL}, \ \forall t \in \Omega^T \tag{26}$$

$$0 \le I_{yz,t}^L \le \overline{I^L} \qquad \forall yz \in \Omega^{TL}, \ \forall t \in \Omega^T \tag{27}$$

Equation (28) determines the suitable limitations on the variable $\Delta V_{yz.t}$.

$$\left|\Delta V_{yz,t}\right| \le (\overline{V} - \underline{V})\left(1 - w_{yz,t}^L\right) \qquad \forall yz \in \Omega^L, \forall t \in \Omega^T \tag{28}$$

Equations (29) and (30) give the amount of power transferred in the network, which is bounded by the limits of the power flow connecting the distribution system to the utility network.

$$-\overline{P_l^M} \le P_{l,t}^M \le \overline{P_l^M} \qquad \forall l \in \Omega^{MG}, \ \forall t \in \Omega^T \tag{29}$$

$$-\overline{Q_l^M} \le Q_{l,t}^M \le \overline{Q_l^M} \qquad \forall l \in \Omega^{MG}, \ \forall t \in \Omega^T \tag{30}$$

The described radiality limitation is an autoreactive constraint for the optimal operation of a distribution network, although there is a possibility that some buses that have suffered damage because of the severe operating conditions (post-flood) cannot be retrieved and will stay in the islanded mode. In such a case, keeping the radial network in the traditional way would force the network to associate healthy hardware to imperfect components and finally bring the system into an unsteady mode. To handle this condition, the complex of buses in the distribution system must be overhauled in each cycle so that those buses that exit from the islands are included in the set.

The abovementioned buses can be included in the procedure of reconfiguration and would follow the radiality limitation. From another viewpoint, if the demand at bus y is energized by the distribution system, then, there is an alternative supply to a critical bus complex in the

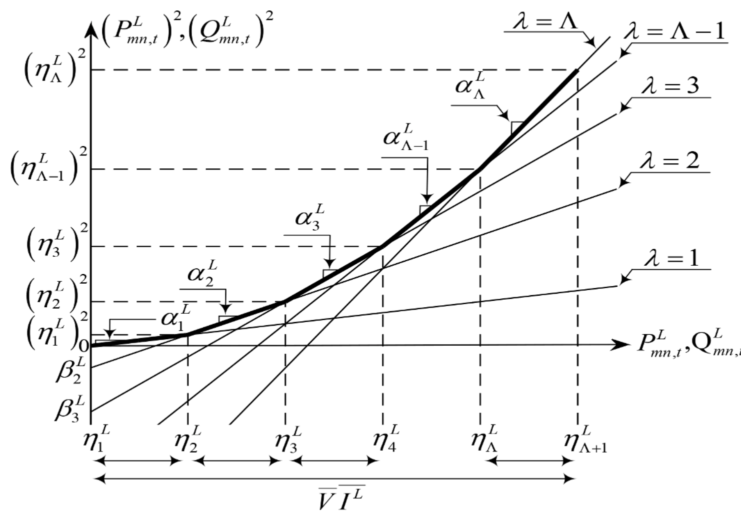

Fig. 2. Conceptual illustration of the relaxed piecewise linear approximation of the quadratic terms.

distribution system. Under such conditions, complete connection of any bus via a node has the ability to be retrieved during the load flow process; thus, buses in the presence of a fault on a permanent line could remain islanded without a distribution system connection mode. These buses are disconnected from the adjacent buses because of the permanent node failures. These buses must be eliminated from the complex of buses in the related distribution system to avoid issues for the radiality limitation of the grid. Hence, the reorganized complex of buses Ω^{B*}_k, that would come across the radiality limit in the distribution system is written as following Eq. (31):

$$\Omega^{B*} = \{y|\exists xy \in \Omega^{TL} OR|\exists xy \in \Omega^{DL}\}; \tag{31}$$

The radiality limitation may be a significant limitation in the typical operation of the electricity distribution system. Within the extraordinary operating mode (such as after a flood), it is evident that a few damaged buses cannot be reestablished and will thus stay islanded. In that case, considering the radiality imperative will constrain the proposed system to associate a significant proportion of the system configuration to completely damaged transport and thereby degrade the framework resilience. To avoid such cases, the radiality constraint should be omitted from the system resilience equations and only be considered in the normal situation. Furthermore, the following constraints Eqs. (32) to (37) are added to the proposed framework to show the radiality constraint for the normal operation case as follows:

$$\sum_{xy\in\Omega^F} w^L_{xy,t} = 1 \qquad \forall y \in \left(\Omega^{BAD} \cup \Omega^{BCD}\right), \quad \forall t \in \Omega^T \tag{32}$$

$$\sum_{xy\in\Omega^L} \theta^L_{xy,t} - \sum_{yz\in\Omega^L} \theta^L_{yz,t} + \theta^M_{y,t} = \theta^D_{y,t} \qquad \forall y \in \Omega^{B*}, \ \forall t \in \Omega^T \tag{33}$$

$$0 \le \theta^L_{yz,t} \le |\Omega^N| w^L_{yz,t} \qquad \forall yz \in \Omega^{DL}, \ \forall t \in \Omega^T \tag{34}$$

$$0 \le \theta^L_{yz,t} \le |\Omega^N| \qquad \forall yz \in \Omega^{TL}, \forall t \in \Omega^T \tag{35}$$

$$0 \le \theta^M_{y,t} \le |\Omega^N| \qquad \forall y \in \Omega^{B*}, \ \forall t \in \Omega^T \tag{36}$$

$$\theta^D_{y,t} = \begin{cases} 1 & \forall y \in \left(\Omega^{BG} \cup \Omega^{BS}\right), \quad \forall t \in \Omega^T \\ 0 & \forall y \notin \left(\Omega^{BG} \cup \Omega^{BS}\right), \quad \forall t \in \Omega^T \end{cases} \tag{37}$$

where $\theta^L_{yz,t}$, $\theta^M_{y,t}$, $\theta^D_{y,t}$ indicate the expected flow of current in the distribution lines, the network and demand, respectively, which are defined in relations (33)–(37). In addition, the radiality of the network will be guaranteed by constraints (33)–(37). It is worth mentioning that the above-mentioned constraints describe a complex of virtual current flows (presented by θ) in order to cover demands on each bus along with the related possible integration alternatives to the distribution system. It is clear that the bus y' of the conventional $\Omega^{B*}(y' \notin \Omega^{B*})$ must be in the islanded mode, indeed, this bus will be retrieved through its own DG or EH battery and MEHs based on the case, which consists of the status of the road, accessible capacity, and the characteristics of the objective functions. This formulation provides a nonconvex and MINLP problem, which is quite hard to resolve and does not ensure an optimal solution, even though the formulation of the first stage of the problem is tractable. Hence, to cope with this issue, the problem under consideration should be changed to the linearized framework.

2.4. Linearization method for the distribution system

Constraints (21)–(24) are the major nonlinearity terms of the previous section, which can be written with new variables to linearize the above equations as following Eqs. (38) and (39):

$$f^L_{mn,t} = \left(I^L_{mn,t}\right)^2 \qquad \forall mn \in \Omega^L, \ \forall t \in \Omega^T \tag{38}$$

$$u_{m,t} = \left(V_{m,t}\right)^2 \qquad \forall m \in \Omega^B, \ \forall t \in \Omega^T \tag{39}$$

Regarding the new definition, the variables in (20)–(26) are updated as following equations (Eqs. (40)–(47)):

$$\sum_{lm\in\Omega^L}\left[P^L_{lm,t} - R_{lm} f^L_{lm,t}\right] - \sum_{mn\in\Omega^L} P^L_{mn,t} + P^G_{m,t} + P^{MEH}_{n,t} - P^{Ch}_{m,t} + P^{Disch}_{m,t} + \sum_{l\in\Omega^{MG}} P^M_{l,t} = P^D_{m,t}$$
$$\forall m \in \Omega^B, \forall n \in \Omega^{MEH}, \forall t \in \Omega^T \tag{40}$$

$$\sum_{lm\in\Omega^L}\left[Q^L_{lm,t} - X_{lm} f^L_{lm,t}\right] - \sum_{mn\in\Omega^L} Q^L_{mn,t} + Q^G_{m,t} + Q^{MEH}_{n,t} + \sum_{l\in\Omega^{MG}} Q^M_{l,t} = Q^D_{m,t} \forall m$$
$$\in \Omega^B, \qquad \forall n \in \Omega^{MEH}, \forall t \in \Omega^T \tag{41}$$

$$u_{m,t} - u_{n,t} = 2\left(R_{mn} P^L_{mn,t} + X_{mn} Q^L_{mn,t}\right) - (Z_{mn})^2 f^L_{mn,t} + \Delta V_{mn,t} \qquad \forall mn$$
$$\in \Omega^L, \forall t \in \Omega^T \tag{42}$$

$$u_{m,t} f^L_{mn,t} = \left(P^L_{mn,t}\right)^2 + \left(Q^L_{mn,t}\right)^2 \qquad \forall mn \in \Omega^L, \ \forall t \in \Omega^T \tag{43}$$

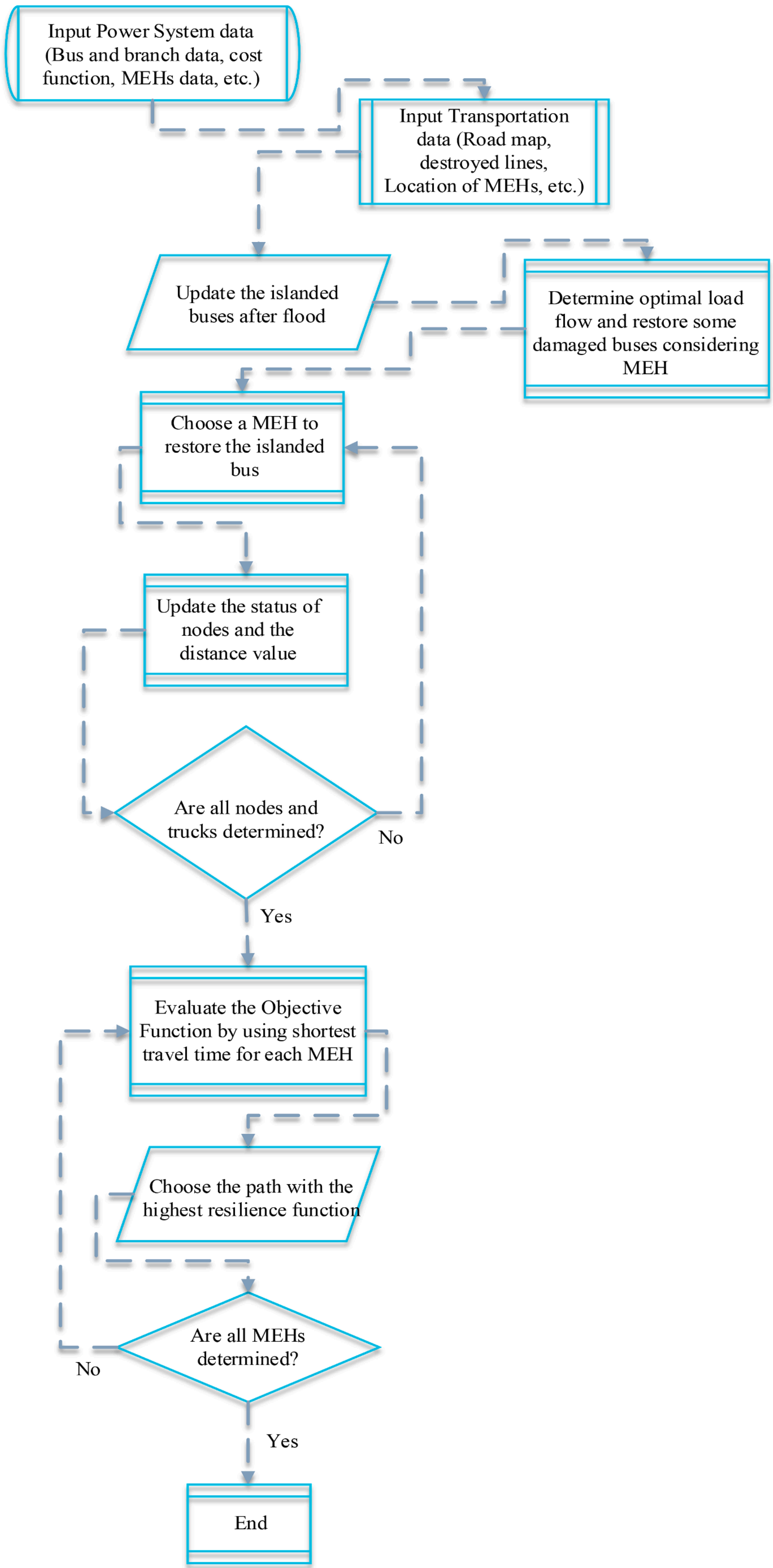

Fig. 3. Overview of the proposed optimization model.

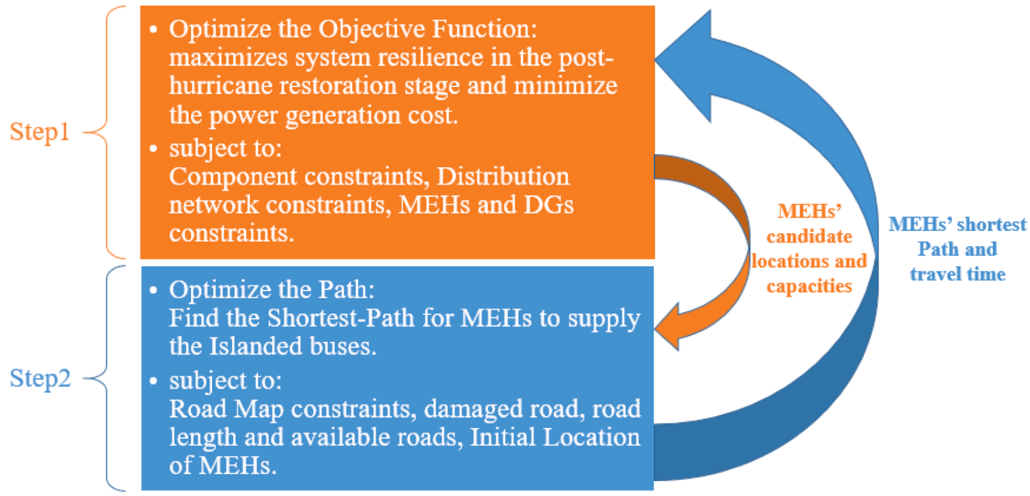

Fig. 4. Interconnection between the proposed algorithm and the optimization framework.

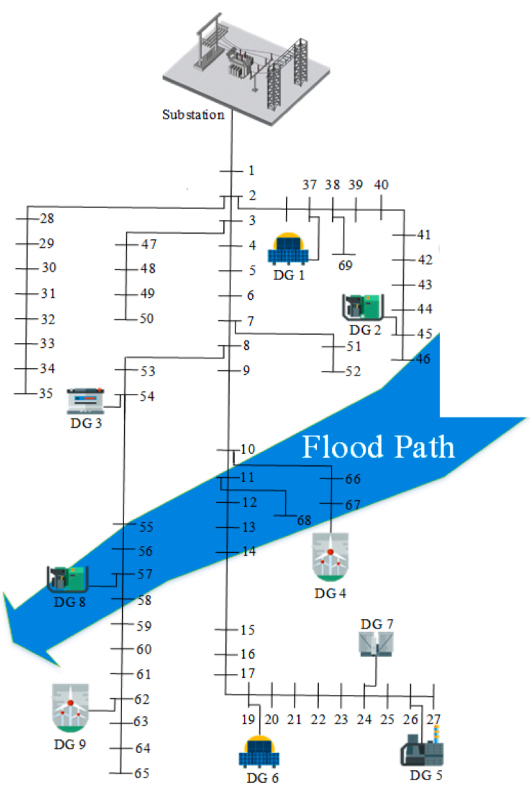

Fig. 5. Representation of the proposed distribution system.

$$(\underline{V})^2 \le u_{m,t} \le (\overline{V})^2 \qquad \forall m \in \Omega^B,\ \forall t \in \Omega^T \tag{44}$$

$$0 \le f^L_{mn,t} \le \left(\overline{I^L}\right)^2 w^L_{mn,t} \qquad \forall mn \in \Omega^{DL}, \forall t \in \Omega^T \tag{45}$$

$$0 \le f^L_{mn,t} \le \left(\overline{I^L}\right)^2 \qquad \forall mn \in \Omega^{TL},\ \forall t \in \Omega^T \tag{46}$$

$$\left|\Delta V_{mn,t}\right| \le \left[(\overline{V})^2 - (\underline{V})^2\right]\left(1 - w^L_{mn,t}\right) \qquad \forall mn \in \Omega^L, \forall t \in \Omega^T \tag{47}$$

By taking into account the above-defined new relation, (21)–(24) can be linearized through a new explanation of the variables. Furthermore, in the rest of this section, the remaining constraint (43) will be defined, because it should be linearized.

Because of the limited range of variation in the magnitude of the bus voltage (typically between 0.9 V^{nom} and 1.1 V^{nom}), the bilinear term $u_{m,t}f^L_{mn,t}$on the left-hand side of constraint (43) can be approximated as Eq. (48):

$$u_{m,t}f^L_{mn,t} \approx (V^{nom})^2 f^L_{mn,t}; \qquad \forall mn \in \Omega^L,\ \forall t \in \Omega^T \tag{48}$$

Moreover, the quadratic terms $(P^L_{mn,t})^2$and $(Q^L_{mn,t})^2$on the right-hand side of constraint (43) are linearized by using a relaxed version of the piecewise linearization method as (Eqs. (49)-(54)):

$$\left(P^L_{mn,t}\right)^2 + \left(Q^L_{mn,t}\right)^2 \approx p^L_{mn,t} + q^L_{mn,t} \qquad \forall mn \in \Omega^L,\ \forall t \in \Omega^T \tag{49}$$

$$p^L_{mn,t} \ge \alpha^L_\lambda P^L_{mn,t} + \beta^L_\lambda \qquad \forall mn \in \Omega^L,\ \forall t \in \Omega^T,\ \forall \lambda = 1,\dots,\ \Lambda \tag{50}$$

$$q^L_{mn,t} \ge \alpha^L_\lambda Q^L_{mn,t} + \beta^L_\lambda \qquad \forall mn \in \Omega^L,\ \forall t \in \Omega^T,\ \forall \lambda = 1,\dots,\ \Lambda \tag{51}$$

$$\alpha^L_\lambda = \left[\left(\eta^L_{\lambda+1}\right)^2 - \left(\eta^L_\lambda\right)^2\right] \Big/ \left[\eta^L_{\lambda+1} - \eta^L_\lambda\right] \qquad \forall \lambda = 1,\dots,\ \Lambda \tag{52}$$

$$\beta^L_\lambda = \left(\eta^L_\lambda\right)^2 - \alpha^L_\lambda \eta^L_\lambda \qquad \forall \lambda = 1,\dots,\ \Lambda \tag{53}$$

$$\eta^L_\lambda = (\lambda - 1)(1/\Lambda)\overline{VI^L} \qquad \forall \lambda = 1,\dots,\ \Lambda \tag{54}$$

In the above formulation, $p^L_{mn,t}$ and $q^L_{mn,t}$ are auxiliary continuous variables, and α^L_λ,β^L_λ and η^L_λ are the necessary linearization parameters.

In comparison with conventional piecewise linearization algorithms, an advantage of the proposed relaxed piecewise linearization method is that it does not employ any auxiliary binary variables. This is a significant benefit because adding an auxiliary binary variable may significantly increase the overall computational burden of the optimization problem. In order to better describe the concept of this idea, Fig. 2 shows the proposed relaxed piecewise linear approximation method for the quadratic terms. As seen in Fig. 2, first, the distance between zero and $\overline{VI^L}$ is broken down into Λ segments. Then, a line with the angle of α^L_λ and the capture of β^L_λ is designated to each segment λ. Finally, the envelope devised by this cluster of lines is employed to approximate the quadratic term.

The proposed linearization is used to provide accurate investigation of the grid and fast development for elements, batteries, and MEHs in a short period of time. Thus, the main goal of this linearization is to have an accurate and fast estimation of the energy not supplied (ENS) and improving the resilience objective function. In this way, some buses in the severely damaged areas may not be appropriate for restoration (either because of technical limitations or damage to the infrastructure) and thus, it may be preferable to leave them uncharged and instead

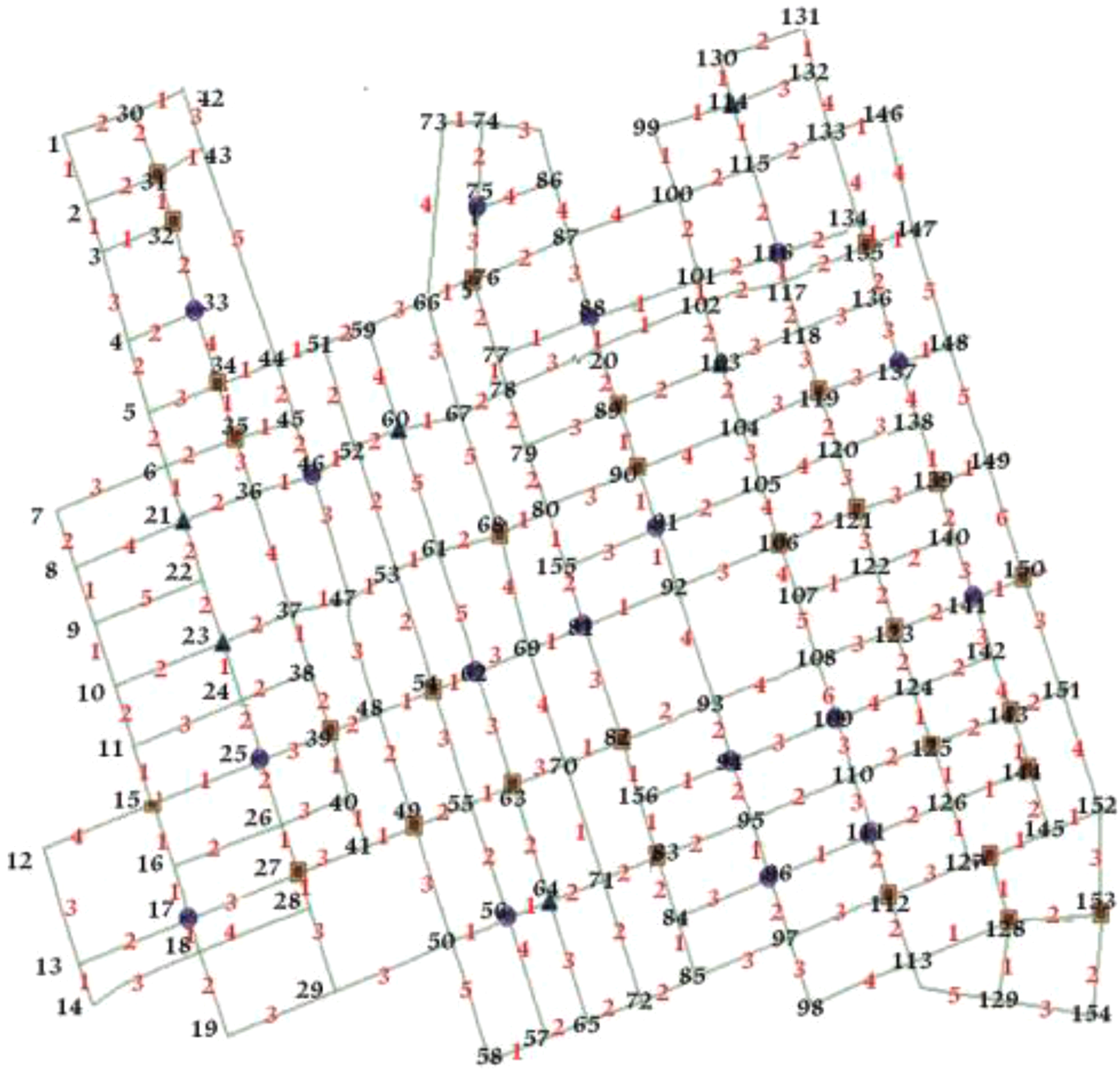

Fig. 6. Road map of the proposed network.

Table 2
Information of destroyed lines, roads, and islanded buses.

Roads out of order on the map	Islanded bus on the distribution system	Destroyed lines on the distribution system
55,68,107,78,95,20,91	11,12,13,56,57,66,67,68	10–11,11–12,11–68,12–13,13–14,56–55,56–57,57–58,66–10,66–67,68–11

Table 3
Information of available trucks.

Truck Number	Active power (kW)	Reactive power (kVAr)	Starting node of the trucks
1	200	150	7
2	250	200	73
3	200	250	149
4	250	200	19

restore loads in the less damaged areas to maximize load restoration. In this situation, the proposed linear model is capable of providing a power flow for a grid with islanded buses, which are potential candidates for power delivery by the MEHs. An overview of the proposed model is shown in Fig. 3.

Table 4
Effect of damaged paths in different cases.

Case	Damaged paths	Destroyed lines	The objective value of resilience problem ($)
1	-	-	345630.79
2	55-56	15-16	312070.63
3	55–56, 66–76	15-16,5-6	310005.15
4	36–46, 66–73, 139–149, 19–29	54–53,2–3,45-46,64–65	301569.58
5	55–56, 66–76, 122–140, 107–122	15–16,5–6,24–25,26–27	309043.96

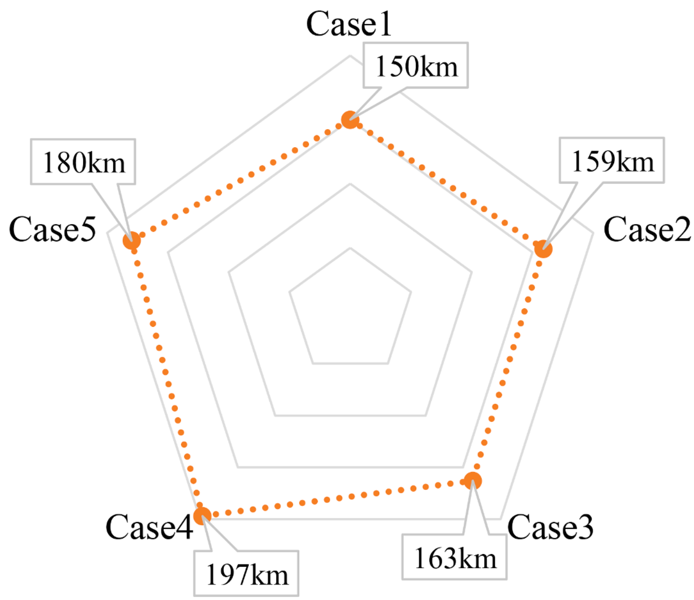

Fig. 7. Total distance traveled by all trucks in each case.

Table 5
Optimal paths of each truck.

Truck Number	Optimal Paths
1	7→6→21→36→46→52→53→61→68
2	73→66→76→77→78
3	149→139→140→122→107
4	19→29→50→56→55

3. Shortest Path Routing Algorithm

With the objective of determining optimal routes for mobile trucks in order to supply the isolated buses that experience a power shortage after a flood, this paper proposes a novel optimization algorithm to find the shortest and undamaged roads [25]. This algorithm is able to calculate the closest path from node (s) to all nodes of the grid in the shortest possible time by considering the transportation routes that are destroyed by the flood. The SPA approach is considered in this study to detect the best direction for handing over MEHs to the isolated buses as well as buses suffering from a power shortage. It should be noted that A* and dynamic programming can also be used in the same approach as other path-finding algorithms. In this respect, the SPA is able to solve the problem of the shortest one-to-all route, simultaneously assessing the shortest direction issue from an applicant node (s) to all the other nodes in the power grid, granted a weighted network (Ω^B, Ω^{TL}, Ω^Δ) with a set Ω^B, the superiority set Ω^{TL}, the weight set Ω^Δ, and characterizing weights C_{ij} for the edge (i, j)$\epsilon\Omega^{TL}$. As suggested above, the big data available before the natural disaster (flood) would guide MEHs to replace their route to the best and suitable points near the flood route for fast handing over to the damaged zones. Hence, the beginning spot of the post-flood is $s\epsilon\Omega^B$. The nodes of appropriate destination are specified in the first step of the optimization framework as expressed in the section 2 of this paper. The buses that should remain islanded cause a supply shortage to feeder service, which should be determined as a linear power flow illustrated in previous section.

Under such a condition, all buses would be able to be retrieved even after an optimal load flow simply by the respective damage intensity arising from flood in the area. In addition, for load restoration by employing mobile trucks (MEHs), all buses have to be considered potential candidates. In order to find the optimal and shortest road routes among all roads, also by taking into account the limitations on the number of mobile trucks and possible destroyed roads to charge the buses, the SPA has to be applied in the second step to cope with this issue. Considering this situation, it will be possible that a number of buses are not available at all because of long distances or destroyed roads. To deal with this problem, two criteria have to be provided for the selection of the most suitable buses for the retrieval of mobile emergency vehicle MEHs: (i) The buses with the shortest route to the mobile trucks' primary position and (ii): the buses with a greater load horizon. It is clear that the proposed strategy would retrieve the buses with the shortest direction and a greater demand via the MEHs. As it has already been shown, there is a situation in which the number of mobile vehicles (truck-mounted MEH) is likely to be lower than the number of MEHs needed by affected buses, and thus, it is possible that only some of them are retrieved according to the shortest route benchmark and the preference. To cope with blocked roads, these paths are eliminated from the set Ω^{TL} in the SPA. In this regard, the weight C_{ij} for the edge (i, j) is assumed as the physical distance between two nodes.

Hence, the following stages are applied to find the optimal direction for handing over MEHs to the destroyed buses:

Stage 1. Select a MEH with the beginning spot $s\epsilon\Omega^B$.

Stage 2. Initialization of the node positions.

a Provide the zero space amount to the node s, and determine it as "Permanent". (The node s turns into (0, pe).)
b Allocate an infinite amount to each node along with its characteristic "Temporary". (The statuses of other nodes are (∞, te).)
c Provide node s as the existing node.

Stage 3. in this stage, both the parameters, the distance and design of the current node, are updated. Allocate i as the current node indicator and after that:

(1) Specify the nodes set Ω^j along with an interim characteristic that can be affected from the current node i through a link (i,j). Update the distance of the aforementioned node. The distance d_j is updated for every node $j\epsilon\Omega^j$ applying the relation as Eq. (55):

$$d_j^{new} = \mathbf{min}\{d_j, d_i + C_{i,j}\} \tag{55}$$

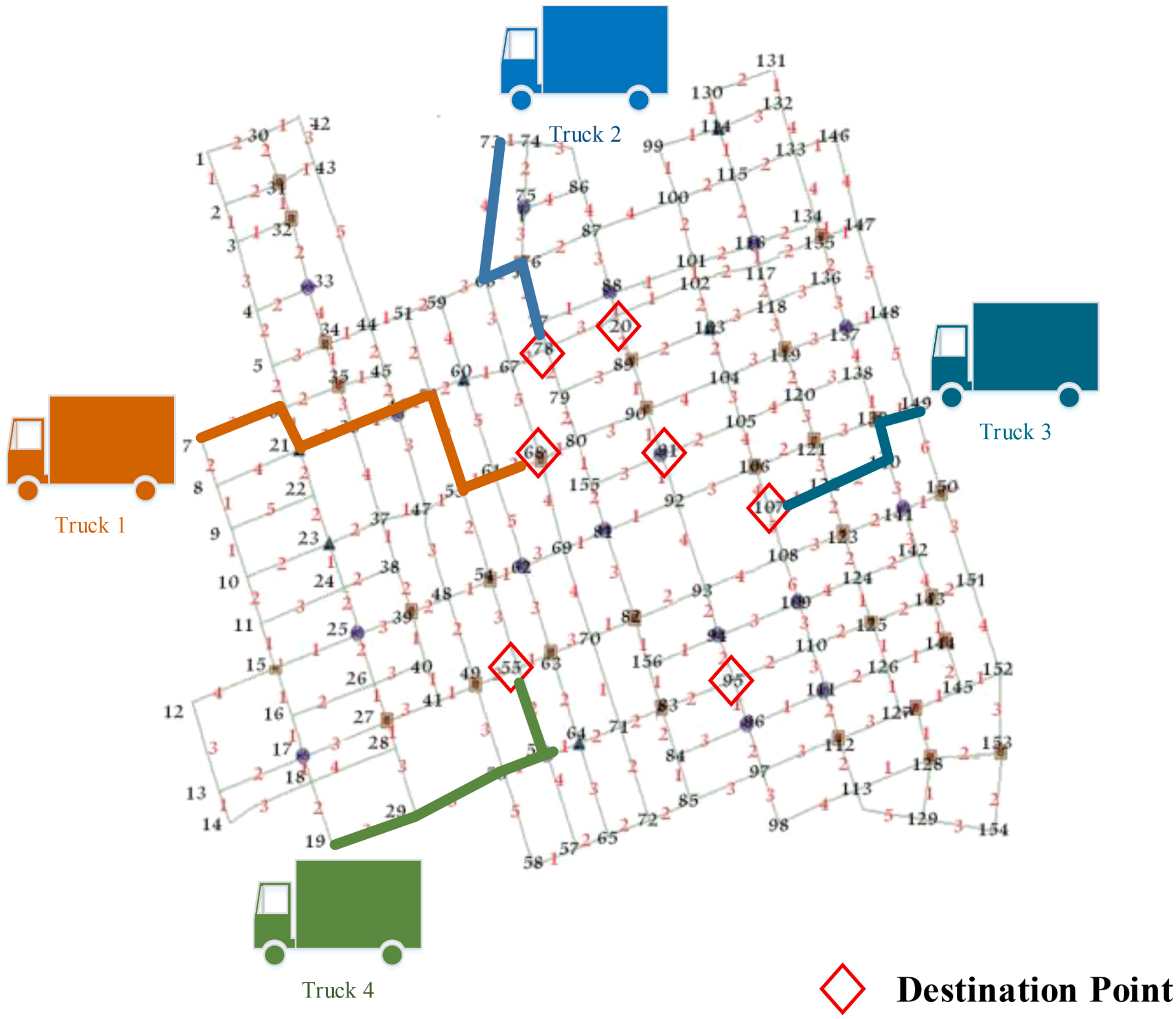

Fig. 8. Representation of optimal paths of the trucks.

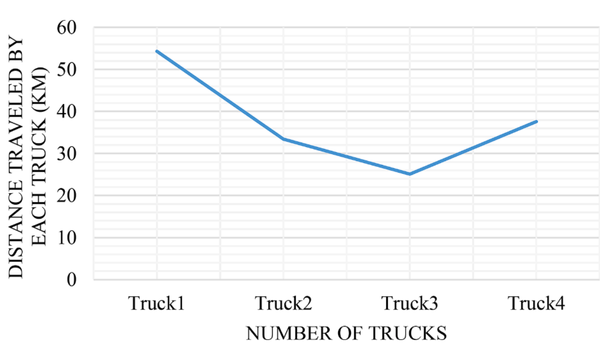

Fig. 9. Comparative distances of each truck.

(2) Confirm a node j that has the smallest space d_j between all nodes $j\epsilon\Omega^j$ and find the Ω^{j*} as Eq. (56):

$$min_{j\epsilon J}\ d_j = d_{j*} \tag{56}$$

(3) In this process, the node j^* will be updated to "Permanent", and this node is determined as the existing node. **Stage 4**. Investigate the closure framework. At this level, the algorithm will be finished (go to stage 5), on the condition that all the aforementioned nodes that are able to reach from node s are continuously considered, otherwise go to stage 3.

Stage 5. Return to step 1, if all the mobile trucks manage to end the algorithm.

Fig. 4 illustrates the interconnection of the proposed algorithm and the optimization model.

4. Simulation Results

The simulations related to the distribution system sample test illustrated in Fig. 5 [26] are represented in this section. The distribution system consists of 68 separator switches and nine DGs. All simulations were carried out simultaneously, in less than 1 s in GAMS and MATLAB software environments. Geographical data and road locations for the sample network are obtained from [27]. Fig. 6 demonstrates the network route map, which includes 154 nodes (black numbers) and 269 sides (edges), in which the red numbers represent the distances between different points of the network (1 unit is equal to 4.18 km). It is assumed that the center of the proposed distribution system is the only approximate point which will face the flood, and points like 55, 68, 107, 78, 95, 20, and 91 will be islanded. Table 2 demonstrates the relation assumed between the islanded points on the road map that are destroyed by the flood and the damaged points on the distribution system. Hence, all

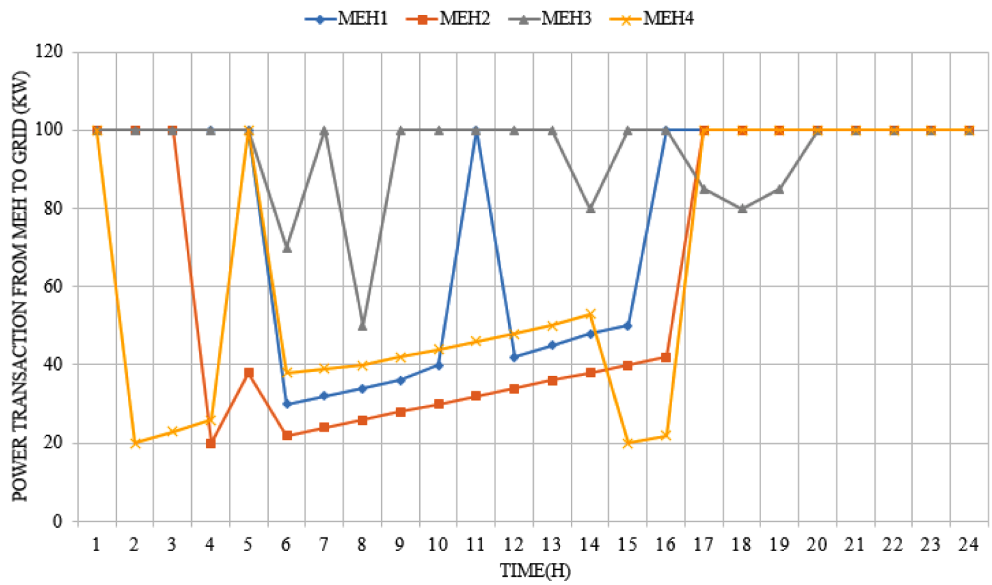

Fig. 10. Power transactions of the MEHs to the grid.

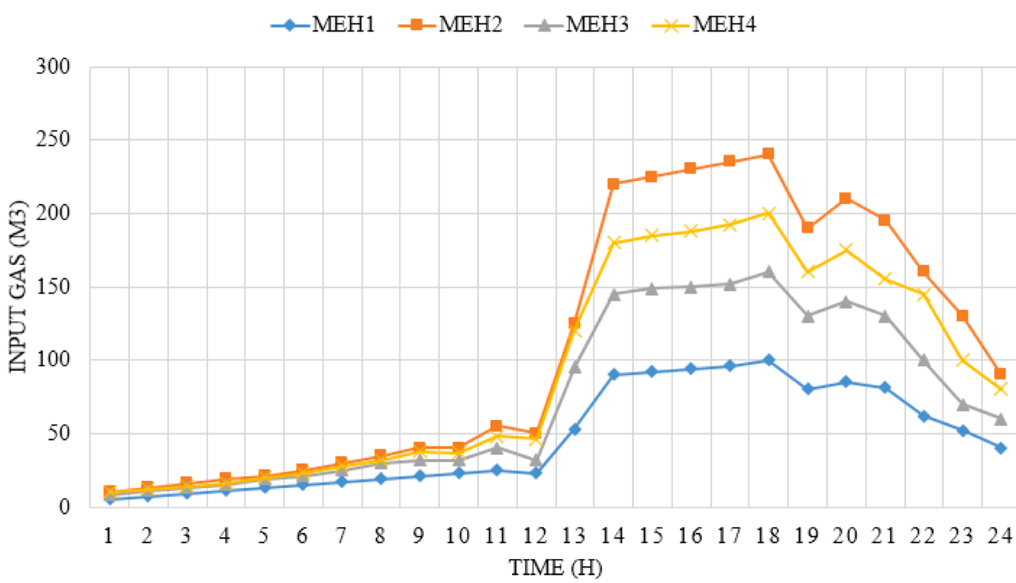

Fig. 11. Input gas of the MEHs.

Table 6
Comparison of resiliency evaluation for different power systems.

Power systems	The objective value of resilience problem($)	Total distance traveled by all MEHs(Km)
16 bus	101257.45	112
33 bus	231795.83	137
69 bus (base case)	345630.79	150
83 bus	395742.02	162

portable EHs installed on the mobile trucks will head to the appropriate locations based on the information received from the satellites, containing meteorological data before the flood event. The information on the portable EHs and their locations is given in Table 3. In this paper, five different cases are considered, in which different routes are destroyed by the flood and cannot thus be chosen by the mobile trucks.

In this way, not only the adverse effects on different paths are considered, but also the effects on power lines in the distribution system destroyed by the severe flood are illustrated in Table 4. As can be seen in Case 1, the value of the objective function of the resilience problem is at the maximum because all the routes and power lines are without any destructions. In comparison with Case 1, the MEHs in Case 2 face damaged paths 55–56 and destroyed lines 15–16, which force the MEHs to drive further to deliver power to the islanded nodes and, in turn, will degrade the resilience objective function. However, this definition cannot be the same for all trucks.

One can conclude that the value of the resilience objective function will decrease if the trucks with EHs have to travel more kilometers to reach the target points in various conditions.

To clarify this, Fig. 7 shows a comparison of the total distances traveled by all trucks in the proposed five different cases. The figure indicates that the longest distance traveled is found in Case 4, being almost 197 km, which is 47 km more than in Case 1, where all the paths are available with no damage. For more clarification regarding the optimization problem, the optimal paths of the trucks that travel to the target points related to the first case are provided in Table 5. It can be seen that the truck number one starts at bus 7 and arrives at bus number 68. For all the considered trucks and their paths, Fig. 8 shows the start and end points of the MEHs. Further, for the first case, the total distance traveled by each MEH is illustrated in Fig. 9. It is worth noting that according to the nearest paths for the trucks and values of consumption loads regarding the aforementioned locations, the points 68, 78, 107, and 55 among seven islanded locations affected by the flood, have been selected by the algorithm. According to the obtained results, the amount of the objective function of the resilience problem will decrease with an increase in the routes traveled by the trucks that carry EHs in different conditions of the network. As a result, optimal ways to supply critical islanded loads are vital and required to improve network resilience and reduce the network expenses after unexpected events.

Fig. 10 shows the power transactions from the considered MEHs to the grid for 24 h after the natural disaster. It can be seen that the MEHs have injected almost 100 kW of power to the grid as some of the electrical energy has to remain in the batteries for critical hours. Further, MEH 3 tends to be used more in the middle of the day because of its availability, shorter distance (see Fig. 9), and sufficient capacity to support the demands connected to its destination point, which are higher than those of the other nodes in the middle of the day. After $t=16$, all the MEHs start injecting power at their maximum value of 100 kW to the increased demand of the loads connected to the target points during the late hours of the day.

Fig. 11 depicts the input gas power of the MEHs within the next 24 h after the natural disaster. As can be seen, this figure shows a plateau during $t=1$ to 12, when the input gas volume is less than 50 m^3. Since then, the input gas increases dramatically until $t=14$. Between $t=14$–18, the input gas power experiences a period of stabilization at almost 225 m^3. The amount of input gas reaches its highest value at t=18, which shows the highest thermal demand of the system compared with the other hours of the day. After a turning point at $t=19$, the input gas shows a downward trend after $t=20$ until the end of the day. A similar behavior can be seen for all the MEHs.

Table 6 shows the resiliency evaluation for different test systems using SPA method with repeated approach.

5. Conclusions

This paper proposed an improved post-flood resilient framework based on mobile energy hubs (MEHs) within a distribution system. The paper concentrated on investigating an effective management framework in order to restore the critical loads of the system in a short period of time after a critical situation when the distribution system experiences a severe flood. Further, a comprehensive model of the distribution system was developed, which incorporated the electricity grid, distributed generators, wind units, solar panels, and the EH to model the proposed system. By using the concept of MEHs, there would be a chance of rehabilitating the system by sending mobile energizing systems to islanded points to heal the system and restore critical loads. In this regard, an effective shortest path algorithm (SPA) approach was used in the system to find the optimal paths for transporting the MEHs in the transportation network toward the target points considering the path destroyed by the flood. Five different cases were considered for a detailed analysis. It was found that the resilience will be decreased if the routes traveled by the trucks are increased in different conditions of the network. It should be noted that the resilience objective function of this paper fluctuates due to the travel time of the trucks carrying the MEHs, which differs according to the number and location of damaged roads. Furthermore, the proposed resilient approach can not only decrease the costs resulting from a sever flood, but also reduce the energy not supplied to consumers. On the other hand, the more paths are destroyed by the flood, the less resilient the system will be because the MEHs should drive longer distances to arrive at the targeted points. Moreover, the mounted MEHs could sufficiently supply both the electrical and thermal demand loads after the flood throughout the day. In addition, it was shown that the proposed mathematics-based SPA as an optimization method could find the optimal routes for driving the trucks in the shortest time possible with a very high accuracy. In this paper, it was assumed that the heat network was completely destroyed after the flood, and the heat consumption of the islanded buses is supplied only by MEHs. Further, the heat network could be an important topic for future research and future studies in this area are thus recommended. Hence, this provides a good starting point for discussion and further research.

CRediT authorship contribution statement

Amid Shahbazi: Investigation, Software, Writing – original draft. **Jamshid Aghaei:** Methodology, Supervision. **Taher Niknam:** Supervision. **Masood Ardeshiri:** Conceptualization. **Abdollah Kavousi-Fard:** Formal analysis. **Miadreza Shafie-khah:** Validation.

Declaration of Competing Interest

The authors declare that they have no known competing financial interests or personal relationships that could have appeared to influence the work reported in this paper.

Acknowledgement

The authors thank Dr. Hanna Niemelä for her assistance with proofreading of the paper and comments that greatly improved the manuscript.

References

[1] J. Lopez, J.E. Rubio, C. Alcaraz, A Resilient Architecture for the Smart Grid, IEEE Trans. Industrial Informatics 99 (2018) 1–8.
[2] R.E. Brown, Flood hardening efforts in Florida, in: Proc. IEEE Power Energy Soc. Gen. Meeting Conversion Del. Elect. Energy 21st Century, 2008, pp. 1–7. Jul.
[3] Nariman L. Dehghani, Yousef Mohammadi Darestani, Abdollah Shafieezadeh, Optimal life-cycle resilience enhancement of aging power distribution systems: A MINLP-based preventive maintenance planning, IEEE Access 8 (2020) 22324–22334.
[4] Amid Shahbazi, Jamshid Aghaei, Sasan Pirouzi, Taher Niknam, Miadreza Shafie-khah, João PS Catalão, Effects of resilience-oriented design on distribution networks operation planning, Electric Power Systems Research 191 (2021), 106902.
[5] Amid Shahbazi, Jamshid Aghaei, Sasan Pirouzi, Miadreza Shafie-khah, João PS Catalão, Hybrid stochastic/robust optimization model for resilient architecture of distribution networks against extreme weather conditions, International Journal of Electrical Power & Energy Systems 126 (2021), 106576.
[6] Mathaios Panteli, Pierluigi Mancarella, The Grid: Stronger, Bigger, Smarter? Presenting a Conceptual Framework of Power System Resilience, Power and Energy Magazine, IEEE 13 (3) (2015) 58–66.
[7] H. Seyedmohsen, B. Kash, E. Jose, A review of definitions and measures of system resilience, Reliability Engineering & System Safety 145 (2016) 47–61. January.
[8] Amirhossein Nasri, Amir Abdollahi, Masoud Rashidinejad, Multi-stage and resilience-based distribution network expansion planning against hurricanes based on vulnerability and resiliency metrics, International Journal of Electrical Power & Energy Systems 136 (2022), 107640.
[9] D. Henry, J. Emmanuel Ramirez-Marquez, Generic metrics and quantitative approaches for system resilience as a function of time, Rel. Eng. & Syst. Safety 99 (2012) 114–122. Mar.
[10] Y. Wang, C. Chen, J. Wang, R. Baldick, Research on resilience of power systems under natural disasters—A review, IEEE Trans. Power Syst. 31 (2) (2016) 1604–1613. Mar.
[11] Wei Zhou, Yuying Wang, Feixiang Peng, Ying Liu, Hui Sun, Yu Cong, Distribution network congestion management considering time sequence of peer-to-peer energy trading, International Journal of Electrical Power & Energy Systems 136 (2022), 107646.
[12] Maosheng Sang, Yi Ding, Minglei Bao, Siying Li, Chengjin Ye, Youtong Fang, Resilience-based restoration strategy optimization for interdependent gas and power networks, Applied Energy (302) (2021), 117560.
[13] Ying Wang, Yin Xu, Jinghan He, Using multiple DGs for distribution system service restoration after extreme events, in: *IEEE Power & Energy Society General Meeting (PESGM)*, IEEE, 2018, pp. 1–5.
[14] Minnan Wang, Jin Zhong, Islanding of systems of distributed generation using optimization methodology, in: IEEE Power and Energy Society General Meeting (PESGM), IEEE, 2012, pp. 1–7.

[15] Gowtham Kandaperumal, Anurag K. Srivastava, Resilience of the electric distribution systems: concepts, classification, assessment, challenges, and research needs, IET Smart Grid 3 (2) (2020) 133–143.
[16] Shunbo Lei, Chen Chen, Hui Zhou, Yunhe Hou, Routing and scheduling of mobile power sources for distribution system resilience enhancement, IEEE Transactions on Smart Grid 10 (5) (2018) 5650–5662.
[17] Saeed Mousavizadeh, Mahmoud-Reza Haghifam, Mohammad-Hossein Shariatkhah, A linear two-stage method for resiliency analysis in distribution systems considering renewable energy and demand response resources, Applied energy (211) (2018) 443–460.
[18] Yin Xu, Ying Wang, Jinghan He, Mingyu Su, Pinghao Ni, Resilience-oriented distribution system restoration considering mobile emergency resource dispatch in transportation system, IEEE Access 7 (2019) 73899–73912.
[19] H. Ahmadi, A. Alsubaie, J.R. Martí, Distribution system restoration considering critical infrastructures interdependencies, in: Proc. IEEE PES General Meeting, National Harbor, MD, USA, 2014, pp. 1–5. Jul.
[20] Jip Kim, Yury Dvorkin, Enhancing distribution system resilience with mobile energy storage and microgrids, IEEE Transactions on Smart Grid 10 (5) (2018) 4996–5006.
[21] Abdollah Kavousi Fard, Mengqi Wang, Wencong Su, Stochastic Resilient Post-Hurricane Power System Recovery Based on Mobile Emergency Resources and Reconfigurable Networked Microgrids, IEEE Access. Vol. 6 (2018) 72311–72326. Nov.
[22] M. Roustaei, T. Niknam, S. Salari, H. Chabok, M. Sheikh, A. Kavousi-Fard, J. Aghaei, A Scenario-Based Approach for the Design of Smart Energy and Water Hub, Energy 116931 (2020).
[23] H. Gao, Y. Chen, S. Mei, S. Huang, Y. Xu, Resilience-Oriented Pre-Flood Resource Allocation in Distribution Systems Considering Electric Buses, Proceedings of the IEEE 105 (7) (2017) 1214–1233. July.
[24] Stuart E. Middleton, Lee Middleton, Stefano Modafferi, Real-Time Crisis Mapping of Natural Disasters Using Social Media, IEEE Intelligent Systems 29 (2) (2014) 1–17. MarApr.
[25] Anna Franceschetti, Dorothée Honhon, Gilbert Laporte, Tom Van Woensel, A shortest-path algorithm for the departure time and speed optimization problem, Transportation Science 52 (4) (2018) 756–768.
[26] Abdollah Kavousi-Fard, Morteza Dabbaghjamanesh, Tao Jin, Wencong Su, Mahmoud Roustaei, An Evolutionary Deep Learning-Based Anomaly Detection Model for Securing Vehicles, IEEE Transactions on Intelligent Transportation Systems (2020).
[27] S.H. Huang, P.C. Lin, Vehicle routing–scheduling for municipal waste collection system under the “Keep Trash off the Ground” policy, Omega 55 (2015) 24–37.